Nano Today 44 (2022) 101497

Contents lists available at ScienceDirect

Nano Today

journal homepage: www.elsevier.com/locate/nanotoday

Large cooperative effects in tunneling rates across van der Waals coupled binary self-assembled monolayers

Yuan Li[a,*,1], Dandan Wang[b,1], Wuxian Peng[a], Li Jiang[b], Xiaojiang Yu[c], Damien Thompson[d,*], Christian A. Nijhuis[b,e,f,**]

[a] Department of Chemistry, Tsinghua University, Beijing 100038, China
[b] Department of Chemistry, National University of Singapore, 3 Science Drive 3, Singapore 117543, Singapore
[c] Singapore Synchrotron Light Source, National University of Singapore, 5 Research Link, Singapore 117603, Singapore
[d] Department of Physics, Bernal Institute, University of Limerick, Limerick, Ireland
[e] Graphene Research Centre, National University of Singapore, 6 Science Drive 2, Singapore 117546, Singapore
[f] Hybrid Materials for Opto-Electronics Group, Department of Molecules and Materials, MESA+ Institute for Nanotechnology and Center for Brain-Inspired Nano Systems, Faculty of Science and Technology, University of Twente, 7500 AE Enschede, The Netherlands

ARTICLE INFO

Article history:
Received 17 October 2021
Received in revised form 8 April 2022
Accepted 23 April 2022
Available online 4 May 2022

Keywords:
Self-assembled monolayers
Cooperative effect
Tunneling
Van der Waals interaction
Molecular diode

ABSTRACT

This paper describes large positive cooperative effects of two orders of magnitude in the tunneling rates across molecular junctions of mixed self-assembled monolayers (SAMs) of rectifying (ferrocenyl undecanethiol $HS(CH_2)_{11}Fc$) and non-rectifying molecules with different terminal groups (11-undecanethiol and its derivatives, denoted as $HS(CH_2)_{11}X$, where X = -H, $-NH_2$ or $-NO_2$). By gradually diluting the surface fraction of $HS(CH_2)_{11}Fc$ in the mixed SAM, it is found that the large positive cooperative effect is only important in the coherent tunneling regime but not in the incoherent tunneling regime. Density functional theory (DFT) shows that the measured cooperative effects in the tunneling rates in these binary systems are caused by Fc—X van der Waals interactions which increase in the order of -H < $-NH_2$ < $-NO_2$. These strong cooperative effects dramatically alter the operation of a molecular diode, further highlighting the importance of taking cooperative effects into account, in this case driven by van der Waals interactions, in the rational design of electronic devices working at tunneling regime.

Introduction

Molecular junctions based on self-assembled monolayers (SAMs), or a single molecule, are widely used to study the mechanisms of charge transport at the molecular level with the aim to generate electronic function at the molecular length scale [1–4]. Often, the mechanisms of charge transport are studied using a physical-organic approach to investigate, for example, how a systematic change in the chemical structure of the SAM precursor, the SAM structure, and/or electrode materials, alters the observed charge transport rates [5–8]. How neighboring molecules affect the tunneling rates in molecular devices, i.e., cooperative effects, has been well-explored theoretically but experimentally only sparsely [9,10]. Consequently, basic questions, including in which charge transport regime cooperative effects are important, have not been experimentally addressed [11]. Large-area junctions based on binary SAMs provide the opportunity to study cooperative effects induced by intermolecular interactions between the two components of the SAM. This paper shows that such intermolecular interactions, in this work dominated by van der Waals interactions, can be used as a tool to control the capacitive coupling between neighboring molecules resulting in additional tunneling pathways that in this case changes the charge transport rates by two orders of magnitude. By using molecular diodes, we determine that cooperative effects are only important in the off-resonant coherent tunneling regime, not in the incoherent tunneling regime. Our results show that cooperative effects are important to consider and can be used to tune the performance not only of molecular diodes, but in principle also other types of molecular devices.

A combination of factors contributes to cooperative effects including molecule–molecule interactions, molecule–electrode

* Corresponding authors.
** Corresponding author at: Department of Chemistry, National University of Singapore, 3 Science Drive 3, Singapore 117543, Singapore.
E-mail addresses: yuanli_thu@tsinghua.edu.cn (Y. Li), damien.thompson@ul.ie (D. Thompson), c.a.nijhuis@utwente.nl (C.A. Nijhuis).
[1] These authors contributed equally to this work

https://doi.org/10.1016/j.nantod.2022.101497
1748-0132/

coupling, and electrostatic effects [10,12–14]. In general, it is challenging to investigate the origin of cooperative effects in single-molecule junctions (neighboring molecules are present since single-molecule experiments are based on dilute monolayers) because the exact structure of the metal–molecule–metal junction cannot be independently verified and often continuously changes during the experiment, particularly in break junctions. Reuter and Ratner et al. [9,10] predicted that cooperative effects should be reflected in the line-shapes of the conductance histograms collected from single molecule junctions, but a large number of other factors (thermal fluctuations, electrode geometry, binding configuration, different conformations, and stochastic molecule–electrode rupture) likely dominate the line-shape of conduction histograms [15].

Junctions based on monolayers allow for detailed independent characterization of the metal–monolayer interface and nowadays various methods are available to form reliable top contacts with monolayers [1,7]. For instance, the group of Chiechi showed that collective electrostatic effects in monolayers with embedded dipoles can be used to alter the energy level alignment of molecular junctions, [16] but depolarization effects are important to consider [17,18]. Trasobares et al. experimentally determined a π–π electronic coupling parameter of 35 meV between ferrocenyl (Fc) functionalized monolayers on nanocrystals, [19] and Dubi proposed that intermolecular interactions could result in dephasing leading to, for example, odd-even effects in the tunneling rates [20]. We have found such odd-even effects in Fc-based molecular diodes although they were supramolecular in origin caused by an odd-even oscillation of 40 meV in the SAM van der Waals packing energy [21]. Although it has been theoretically shown that cooperative effects depend strongly on the monolayer density, this is very difficult to control in experiments because dilute monolayers suffer from defects, or different (lying-down) phases form.

These examples showcase that cooperative effects may be electronic or supramolecular in nature and highlight the challenge of elucidating the underlying mechanism of such effects in molecular tunnel junctions. For example, in principle, cooperative effects cannot improve transmission at resonance when the conduction channel is completely open for coherent tunneling, and are therefore expected to be important in the off-resonant tunneling regime [22,23]. Here we show that it is possible to tune the cooperative effects in molecular tunnel junctions based on binary SAMs of ferrocenyl alkanethiolates ($S(CH_2)_{11}Fc$, Fc = ferrocenyl) and $S(CH_2)_{11}X$ with X = -H, $-NO_2$, $-NH_2$ by changing the ratio of the two components and the chemical structure of the terminal group X of the diluent. We found a strong positive cooperative effect resulting in an increase in the tunneling rate of two orders of magnitude. These junctions are molecular diodes that switch their mechanism of charge transport between coherent and incoherent tunneling (when the highest occupied molecular orbital (HOMO) is in resonance) depending on the bias polarity, and positive cooperative effects were only found in the off-resonant tunneling regime in agreement with the theory predictions in ref [10]. Based on detailed complementary SAM characterization, we found that all SAMs have an indistinguishable supramolecular structure, and the results from density functional theory (DFT) calculations indicate that the capacitive coupling between Fc—X is dominated by van der Waals packing, which is primarily responsible for the observed changes in the electrical properties of the junctions.

Results and discussions

Scheme 1 shows the structure of our junctions with binary SAMs of $S(CH_2)_{11}Fc/S(CH_2)_{11}X$ (X = -H, $-NO_2$, $-NH_2$), which we use to investigate how the Fc—X interactions affect the tunneling rates in terms of current densities (J in A cm^{-2}) and the rectification ratio R ($= |J(V_{fwd})/J(V_{rev})|$, with V_{fwd} = forward bias; V_{rev} = reverse bias) as a function of the mole fraction of $S(CH_2)_{11}Fc$ on the surface $\chi_{Fc,surf}$ defined as $\chi_{Fc,surf} = \frac{\Gamma_{Fc}}{4.5 \times 10^{-10} \text{mol/cm}^2}$, where Γ_{Fc} is the surface coverage of Fc with 4.5×10^{-10} mol cm^{-2} for full surface coverage. The advantage of using $S(CH_2)_{11}Fc$ SAMs is that they can be readily characterized with wet electrochemistry. For instance, Chidsey et al. [24] studied binary SAMs of $S(CH_2)_mCO_2Fc/S(CH_2)_nCH_3$ and found that the components segregate resulting in heterogeneous SAMs for $m \neq n$, but homogeneous SAMs can be obtained for $m = n$. We used $m = n = 11$ in our experiments to minimize phase segregation and modulate the Fc—X coupling strength by changing the magnitude of the dipole of X or the $S(CH_2)_{11}Fc/S(CH_2)_{11}X$ ratio.

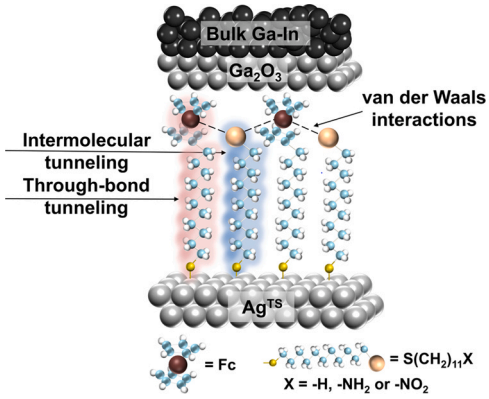

Scheme 1. Schematic illustration of the junctions with mixed SAMs of $S(CH_2)_{11}Fc/S(CH_2)_{11}X$, where X = -H, $-NH_2$ and $-NO_2$. The junctions were formed with GaO_x/EGaIn (oxide layer is roughly 0.7 nm) top-electrodes [31] and template-stripped silver (Ag^{TS}) bottom-electrodes that supported the SAMs. [32] The dashed lines indicate the intermolecular interactions between Fc and X. Two kinds of tunneling pathways are indicated by color: through-bond tunneling in red and the path arising from intermolecular tunneling in blue.(For interpretation of the references to colour in this figure, the reader is referred to the web version of this article.)

Kong et al.[25,26] showed that the value of R of junctions with SAMs of a 4′-methyl-2,2′-bipyridyl (BIPY) moiety of the form $S(CH_2)_{11}BIPY$ could be reduced from 85 to unity by diluting the SAMs with $S(CH_2)_nCH_3$ (n = 7, 9, 15, 17), but in these junctions cooperative effects could not be studied due to interfacial defects. Katsouras et al. [27] studied junctions with mixed SAMs of $S(CH_2)_{11}CH_3/S(CH_2)_{17}CH_3$ and concluded that the electrical resistance of these mixed SAMs increases exponentially with the average thickness of the SAMs. Junctions with binary SAMs have also been used to improve photoswitching, [28] or the electrical stability,[29] of junctions, or to control charge transport in the inverted Marcus region [30]; these studies, however, did not consider the possibility of intermolecular charge transport pathways between the two components of the SAMs.

Electrochemical characterization of the SAMs

The SAM precursors were synthesized using known procedures (see SI). The mixed SAMs were derived from solutions of $S(CH_2)_{11}Fc/S(CH_2)_{11}X$ with the fraction of $HSC_{11}Fc$ in solution, $\chi_{Fc,sol}$ ranging from 0 to 1 following previously reported procedures (see SI). We used template-stripped Au [32] (Fig. S2) to support the SAMs and characterized the SAMs by cyclic voltammetry to determine the values of $\chi_{Fc,surf}$. Fig. 1a-c shows the cyclic voltammograms (CVs) for mixed SAMs at different $\chi_{Fc,sol}$ with scan rate of 1.0 V s^{-1}. The surface coverage of the Fc units, Γ_{Fc} (in mol/cm^2), was determined with Eq. 1.

$$\Gamma_{Fc} = Q_{tot} / nFA \quad (1)$$

where Q_{tot} is the total charge obtained by integration of the anodic wave, n is the number of electrons involved in the redox reaction (here $n = 1$), F is Faraday constant (F = 96,485 C mol^{-1}), and A

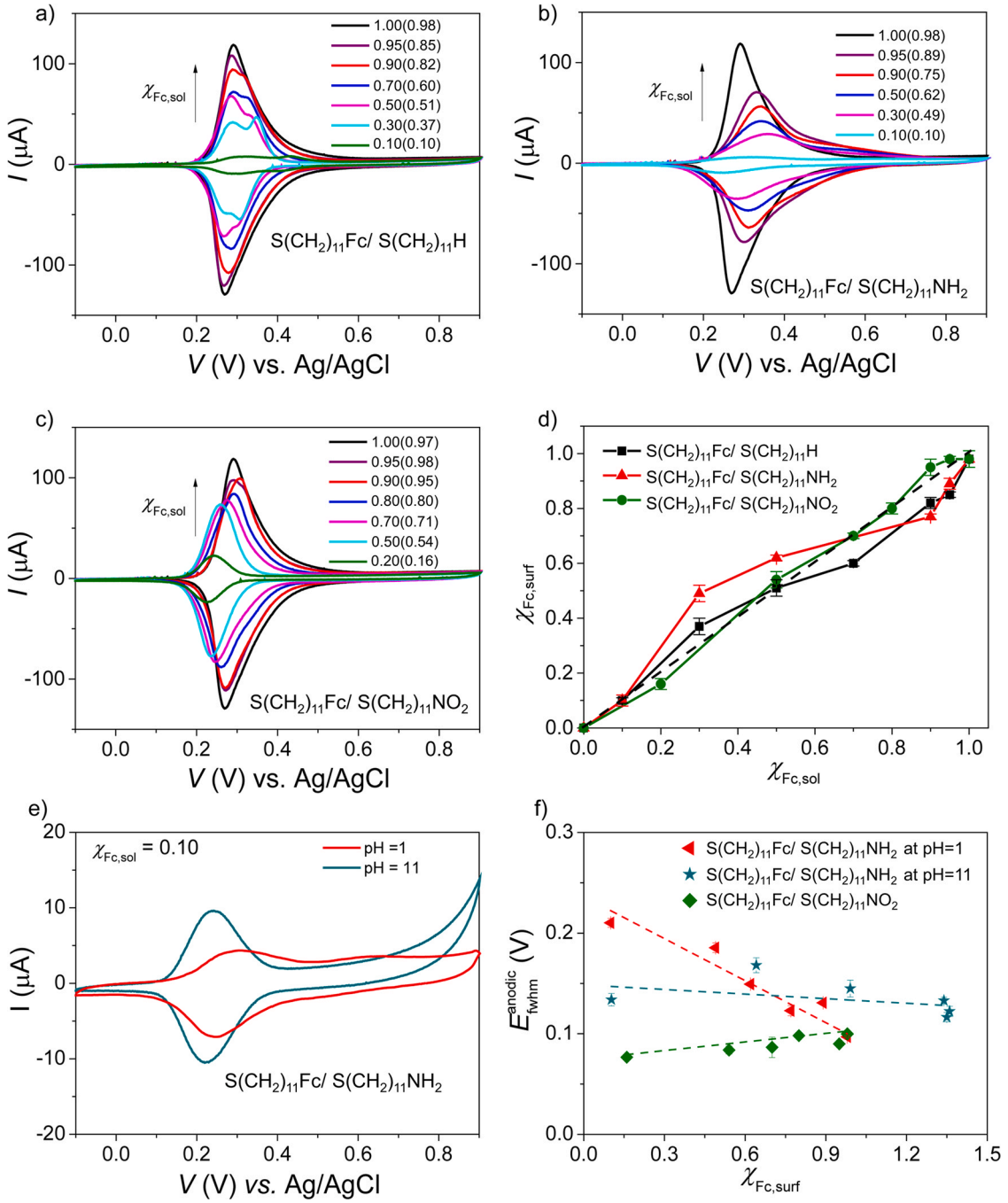

Fig. 1. CV of mixed SAMs $S(CH_2)_{11}Fc/S(CH_2)_{11}X$ for different values of $\chi_{Fc,sol}$ for (a) X = -H, (b) X = $-NH_2$ and (c) X = $-NO_2$. All measurements were carried out with aqueous 1.0 M $HClO_4$ as the electrolyte at a scan rate of 1.0 V s^{-1}. The numbers in parentheses are $\chi_{Fc,surf}$ corresponding to each $\chi_{Fc,sol}$. d) Plot of $\chi_{Fc,surf}$ as a function of $\chi_{Fc,sol}$ for the three mixed SAM systems. The dashed line indicates $\chi_{Fc,sol} = \chi_{Fc,surf}$. The solid lines are visual guides. e) CV of mixed SAMs $S(CH_2)_{11}Fc/S(CH_2)_{11}NH_2$, where $\chi_{Fc,sol}$ = 0.10 on Au^{TS} at a scan rate of 1.0 V s^{-1} in aqueous 1.0 M $HClO_4$ as electrolyte at pH = 1 (red) and in 1.0 M $NaClO_4$ at pH = 11(blue). f) E_{fwhm} as a function of $\chi_{Fc,surf}$ for $S(CH_2)_{11}Fc/S(CH_2)_{11}X$ where X = $-NH_2$ and $-NO_2$. The dashed line is a visual guide. The error bars represent the standard deviations determined from three different experiments.(For interpretation of the references to colour in this figure, the reader is referred to the web version of this article.)

is the surface area of the working electrode in contact with the electrolyte (A = 0.33 cm^2). Fig. 1d shows the relation between $\chi_{Fc,surf}$ and $\chi_{Fc,sol}$. We obtained $\Gamma_{Fc} = (4.40 \pm 0.12) \times 10^{-10}$ mol cm^{-2} for $\chi_{Fc,sol}$ = 1; this value is consistent with previously reported values and the theoretical value of 4.5×10^{-10} mol cm^{-2}[24]. This agreement helps us to confirm our SAM is truly monolayer.

When the Fc SAMs are diluted with $S(CH_2)_{11}H$, a second peak appears which indicates that the Fc units are in at least two distinct electrochemical environments [33,34]. The peak splitting is the result of Fc units interacting with other Fc units and with the alkyl chains for $\chi_{Fc,sol} > 0.1$, resulting in partially-buried Fc units and units that are directly exposed to the electrolyte as explained by us previously [35]. Peak splitting was not observed for the other binary SAMs which indicates that the Fc units were all in the same electrochemical environments likely imposed by much stronger Fc—X interactions for X = NO_2, NH_2. The weak Fc—CH_3 interaction is also reflected in the constant peak anodic potential, E_{pa}, as function of $\chi_{Fc,sol}$ (though a small anodic shift can be seen for $\chi_{Fc,sol} > 0.3$). For the SAMs with X = NH_2, we find a maximum anodic shift of E_{pa} of 71 meV, and for X = NO_2 a maximum cathodic shift of 48 meV. These

Table 1
Measured properties of the mixed SAMs.

$SC_{11}Fc/SC_{11}X$	$\chi_{Fc,sol}$	$\chi_{Fc,surf}$ (CV)[a]	$\chi_{Fc,surf}$ (XPS)[b]	Γ ($\times 10^{-10}$ mol/cm^2)[b]	d[c] (nm)	α[d] (º)	R (σ_{log}[e])
X = -H	1.00	1.00	1.00	4.45	1.8 ± 0.2	53 ± 2	1.0×10^2 (0.43)
	0.90	0.82	0.87	7.89	1.8 ± 0.2	50 ± 2	70.2 (0.33)
	0.50	0.51	0.50	9.66	1.7 ± 0.2	53 ± 2	28.6 (0.42)
	0.10	0.10	0.13	9.10	1.7 ± 0.2	52 ± 2	6.8 (0.21)
X = -NH_2	0.90	0.75	0.91	9.76	1.8 ± 0.2	50 ± 2	14.5 (0.54)
X = -NO_2	0.90	0.95	0.84	9.34	1.8 ± 0.2	54 ± 2	4.3 (0.54)

[a] Determined from CV.
[b] Determined from ARXPS, the error for $\chi_{Fc,surf}$ is about 0.05 estimated from the fitting error of the Fe $2p_{3/2}$ XPS spectra. The error for Γ is about 0.1 estimated from both the fitting error of the Fe $2p_{3/2}$ and S $2p$ spectra.
[c] The error bar reflects fitting errors and angular misalignment due to sample mounting.
[d] The error is due to fitting and instrumental error.
[e] The σ_{log} is the log-standard derivation.

results indicate that Fc—X interactions for these two binary SAMs are much stronger than in binary SAMs with X = H (see Supporting Information for all CVs and a detailed analysis).

Since the SAMs with amine functionalities are basic, they could be partially protonated under ordinary laboratory conditions. Therefore, we recorded CVs using 1.0 M aqueous $NaClO_4$ with pH = 11, or $HClO_4$ with pH = 1, as the electrolyte. In basic electrolyte (Fig. 1e), -NH_2 is in its neutral form and we find that the peak separation ΔE_p ($= E_{pa}$-E_{pc}) is close to 0 mV when $\chi_{Fc,sol} = 0.10$. In acidic electrolyte, -NH_3^+ is formed at the monolayer surface and the peak oxidation potential increases by 62 meV and ΔE_p increases to 58 mV for $\chi_{Fc,sol} = 0.10$. These observations suggest that electrostatic repulsion between Fc^+ and NH_3^+ makes it more difficult to oxidize Fc [36].

To determine whether the Fc—X interactions are attractive or repulsive, we investigated the full width at half maximum (E_{fwhm}) of the oxidation wave using the Laviron approach [37] where the value of E_{fwhm} is defined by the parameter $\upsilon G\theta_T$ as follows

$$E_{fwhm}^{1/2} = \frac{RT}{F}\left(\ln\frac{f}{1-f} + \upsilon G\theta_T\beta(1-2f)\right) \text{where} \beta = \left(\frac{2-\upsilon G\theta_T}{4-G\theta_T}\right)^{1/2} \quad (2)$$

where G is the sum of all possible intermolecular interactions. $f = \theta_o/\theta_T$ and $1\text{-}f = \theta_R/\theta_T$ where $\theta_T = \theta_o + \theta_R$ is the total fractional coverage of the redox-active species. This approach allows us to qualitatively determine whether the Fc—X interaction is attractive or repulsive by examining the $\upsilon G\theta_T$ [38,39]: in case of $\upsilon G\theta_T > 0$, the interaction is predominated by lateral attractive interaction resulting in narrow (< 90 mV) redox wave; in case of $\upsilon G\theta_T < 0$, the interaction is predominated by lateral repulsive interaction resulting in broad (> 92 mV) redox waves; in case of $\upsilon G\theta_T = 0$, the interaction is neutral and the E_{fwhm} is 91 mV (at 25 °C). Fig. 1 f shows that for X = -NO_2, the values of E_{fwhm} decrease from 100 mV to 77 mV as $\chi_{Fc,surf}$ decreases, which indicates that $\upsilon G\theta_T > 0$ and the Fc—NO_2 interaction is attractive [40]. Note that the analysis from E_{fwhm} indicates the Fc—X interactions when Fc is oxidized to Fc^+ in the electrochemical environment. This attractive Fc—NO_2 force could also explain the cathodic shift of the E_{pa} since the Fc^+ units are stabilized by the neighboring NO_2 groups. On the other hand, for X = -NH_2, the values of E_{fwhm} increase as $\chi_{Fc,surf}$ decreases at both pH = 1 and 11 with $E_{fwhm} > 100$ mV. These observations indicate that the Fc—NH_2 interaction is repulsive. At pH = 1, the NH_2 terminus is protonated to -NH_3^+ resulting in strong electrostatic repulsion when Fc is oxidized to Fc^+, leading to steeper increase in E_{fwhm} as $\chi_{Fc,surf}$ decreases (data in red) than for those values of E_{fwhm} measured at pH = 11 (data in blue).

Supramolecular structure of the binary SAMs

As mentioned in the introduction, subtle changes in the supramolecular structure of $SC_{11}Fc$ SAMs can have large effects on the measured tunneling rates across these SAMs [5]. Therefore we determined the $\chi_{Fc,surf}$ and total surface coverage Γ, the thickness of the SAM d_{SAM}, and the tilt angle of the Fc units α (in °) with respect to the surface normal, using angle resolved X-ray photoemission spectroscopy (ARXPS) and near edge X-ray absorption fine structure spectroscopy (NEXAFS) of SAMs of $S(CH_2)_{11}Fc/S(CH_2)_{11}H$ with $\chi_{Fc,sol}$ = 1.00, 0.90, 0.50, 0.1, and $S(CH_2)_{11}Fc/S(CH_2)_{11}X$ for X = -NO_2 or -NH_2 with $\chi_{Fc,sol} = 0.90$ (See SI). The results of $\chi_{Fc,surf}$, d_{SAM}, and α are given in Table 1. From Table 1 we make the following three observations: 1) the values of $\chi_{Fc,surf}$ extracted from XPS agree with those determined from CV, 2) the values of d do not vary much as $\chi_{Fc,sol}$ decreases from 0.9 to 0.1, and 3) the values of α for all mixed SAMs are independent of $\chi_{Fc,sol}$ and the terminal group X. These high quality mixed SAMs allow us to explore the relationship between corporative effect and Fc—X interactions without interference factors such as defects in molecular packing or charge leakage. From these results we conclude that supramolecular structure of the densely packed SAMs with similar α is well-controlled and independent of X with SAMs organized in a well-defined standing-up phase with similar thickness d and Γ.

Charge transport across mixed SAMs

The junctions were formed with the binary SAMs supported by ultra-flat template-stripped silver (Ag^{TS}) electrodes [32] and Ga_2O_3/EGaIn top contacts using previously reported methods.[21] We collected and analyzed statistically large sets of J(V) data (456–528 traces for each type of junction) following previously reported procedures and the details are given in the Supporting Information. [21,41] Figs. 2a, 2c and 2e, show the Gaussian log-average of the absolute values of J, $< \log_{10}|J| >_G$, as a function of the applied bias V. Note that for $\chi_{Fc,sol} = 0$, d_{SAM} was about 0.36 nm shorter than the binary SAM of $S(CH_2)_{11}Fc/S(CH_2)_{11}H$ (See Table S5) causing the increase in the values of J in Fig. 2b. Fig. 3d shows the values of R vs. $\chi_{Fc,surf}$. The most striking result is the sharp decrease in R from 1.0×10^2 to unity with decreasing $\chi_{Fc,surf}$ for X = NH_2 or NO_2. In other words, dilution of the SAMs with $S(CH_2)_{10}CH_3$ results in a gradual decrease of R while dilution with $S(CH_2)_{11}NO_2$ results in a steep decay of R. For instance, $R = 1.0\times10^2$ for junctions with $\chi_{Fc,sol} = 0.95$, for $\chi_{Fc,surf} = 0.80$ with diluent X = CH_3 and, thus, is essentially the same as for $\chi_{Fc,surf} = 1$. In sharp contrast, R decreases to 14.5 for $\chi_{Fc,surf}$ = 0.75 ($\chi_{Fc,sol} = 0.90$), with X = NH_2. For X = NO_2, the value of R is only 4.3 for $\chi_{Fc,surf} = 0.95$ ($\chi_{Fc,sol} = 0.90$) and drops to unity for $\chi_{Fc,surf} = 0.71$ ($\chi_{Fc,sol} = 0.70$).

Interestingly, Figs. 2b, 2d and 2f show that the values of J at negative bias (or forward bias when the diodes are turned on) are nearly independent of the composition of the binary SAMs while the opposite is true for the values of J at positive bias (or reverse bias when the diodes are turned off and only a leakage current flows across the junction). The mechanism of rectification for the Fc-

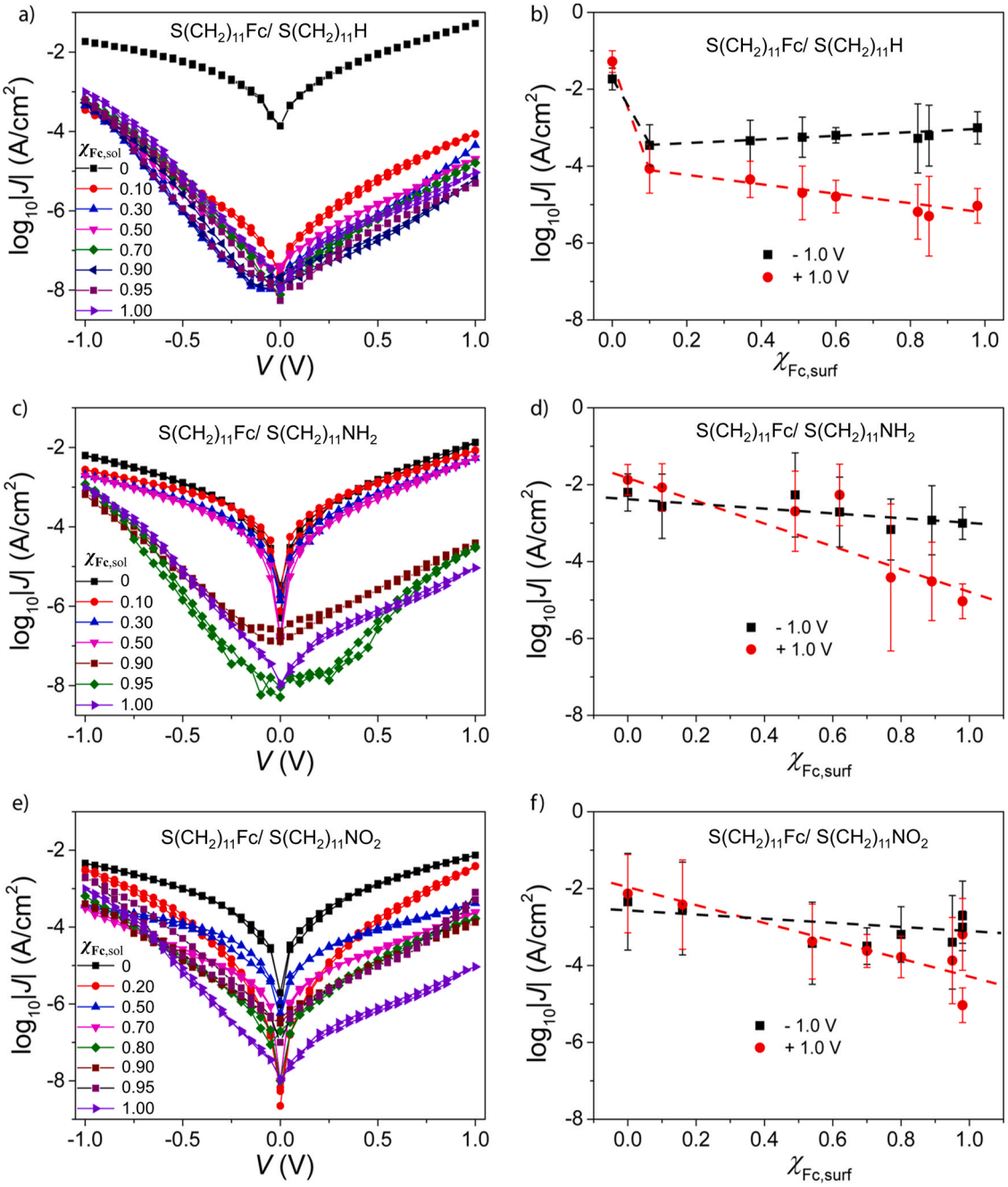

Fig. 2. The $< \log_{10}|J| >$ (V) curves for junctions of mixed SAMs $S(CH_2)_{11}Fc/S(CH_2)_{11}X$ and the values of $< \log_{10}|J| >$ at + 1.0 and − 1.0 V for X = -H (a and b), X = -NH_2 (c and d), and X = -NO_2 (e and f) as a function of $\chi_{Fc,surf}$. The dashed lines are guides for the eyes.

diodes has been reported elsewhere.[5,42] At negative bias, the highest occupied molecular orbital (HOMO) – which is centered at the Fc unit – falls in the bias window. Temperature dependent measurements have shown that the mechanism of charge transport is incoherent tunneling where the Fc acts as a hopping center. Therefore, we conclude that in the incoherent tunneling regime cooperative effects are negligible because the charge transport channel is already completely open since the HOMO falls in the bias window (following the same reasoning as in ref [21]). At positive bias, the HOMO does not fall in the bias window and so the mechanism of charge transport is dominated by a one-step off-resonant coherent tunneling process. Therefore, we conclude that cooperative effects are important in the off-resonant tunneling regime and that the capacitive coupling between Fc and X provides additional tunneling pathways leading to an increase in the measured current across the junction.

The Fc—X interaction

To study the nature of the Fc—X interactions, we performed DFT calculations (Supporting Information Section S11) of the binary SAMs with a ratio of $S(CH_2)_{11}Fc/S(CH_2)_{11}X = 2:1$, or $\chi_{Fc,surf} = 0.67$. The data in Table 2 show that the interaction between the molecules in the mixed SAMs is purely van der Waals's driven. Non-dispersion-corrected, conventional DFT gives positive, or repulsive electronic interactions that miss the van der Waals forces as previously observed also for, *e.g.*, benzene dimers and base pair stacks [43]. This reflects the systematic failure, or inability, of commonly-used DFT

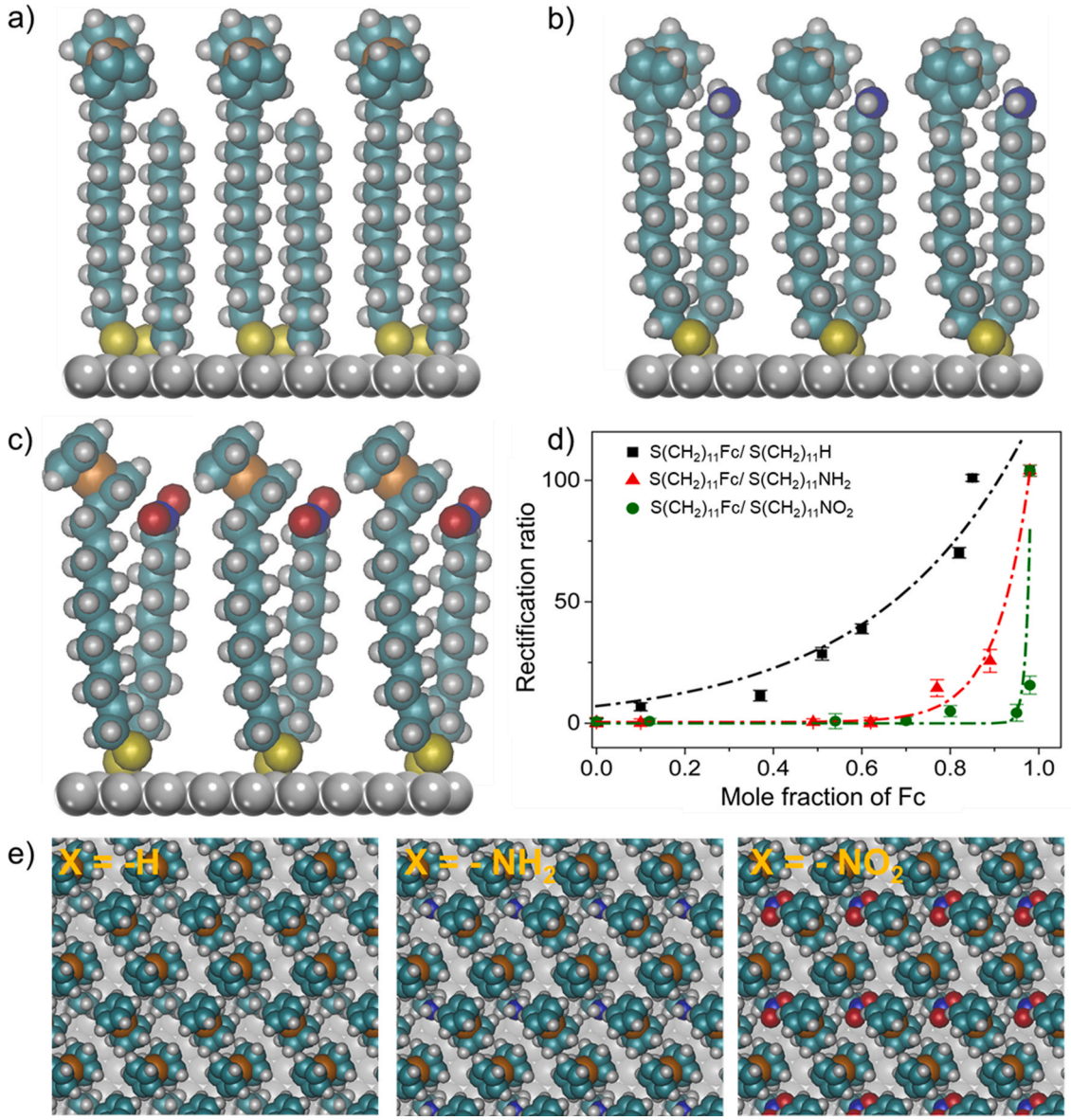

Fig. 3. Illustrative models of the binary SAMs adsorbed on Ag (111) with a surface ratio of $S(CH_2)_{11}Fc/S(CH_2)_{11}X = 1:1$, when X = H (a), NH_2 (b) and NO_2 (c). d) *R* measured as a function of $\chi_{Fc,surf}$ for the junctions with the three types of binary SAMs. The dashed curves are a guide to the eyes. (e) Views down on the computed mixed SAM structures with mole fraction of Fc = 0.67 and X = H (left), NH_2 (middle), and NO_2 (right).

Table 2
Calculated energies of intermolecular interactions[a].

$S(CH_2)_{11}Fc/S(CH_2)_{11}X$	Electronic (meV/molecule)	van der Waals (meV/molecule)	Total (meV/molecule)[b]
X = -H	+ 598	-987	-389
X = $-NH_2$	+ 336	-1479	-1112
X = $-NO_2$	+ 1071	-1966	-895

[a] Repulsive forces are indicated with "+" and attractive forces with "-".
[b] Sum of electronic and van der Waals interactions.

functionals such as PBE to describe long-range dispersion interactions, [43] and so van der Waals's corrections are required to correctly predict the dispersion-driven formation energies of strongly-bound complexes with weak or repulsive electronic interactions. The total energy of the intermolecular interactions, that is electronic plus van der Waals interactions (Table 2), suggest that Fc—X interactions are attractive, and upon replacing X = -H with $-NH_2$ or $-NO_2$ the attractive interactions are at least doubled. Therefore, the van der Waals interactions, as the attractive interactions, dominate the Fc—X interactions in our binary SAM system (Fig. 3e). Interestingly, these calculations show the van der Waals energy follows the $-H < -NH_2 < -NO_2$ trend, which is consistent with the trend of the decrease in *R* in Fig. 3d (or increase of the cooperative effect in the current at positive bias, Fig. 2). By simply doubling Fc—X van der Waals interactions (i.e., replacing H with NO_2), the values of *R* could decay from 100 toward unity even with very small amounts of diluent. The computed DFT structures confirmed zero electronic overlap (charge sharing) between the neutral Fc and X groups, with the contact purely van der Waals in nature. Interestingly, neither the electronic component nor the total energy of the Fc—X interaction follows the measured trend in device performance and, therefore, we conclude that the van der Waals component drives the cooperative effects in our junctions.

Cooperative effect of two orders of magnitude

The large cooperative effect can be clearly seen by comparing the values of *J* at + 1.0 V for junctions with $\chi_{Fc,sol} = 0.90$. For junctions

with $S(CH_2)_{11}Fc/S(CH_2)_{11}X$ with X = -H, for $\chi_{Fc,surf}$ = 0.82 the cooperative effect is the weakest and $\log(J(A\ cm^{-2}))$ = −5.23 (Fig. 2b). In case of X = -NO_2, for $\chi_{Fc,surf}$ = 0.95 the value $\log(J(A\ cm^{-2}))$ = −3.72 (Fig. 2f) is 32 times larger than that for the same junctions with X = -H. The cooperative effect is intermediate for X = -NH_2 with $\chi_{Fc,surf}$ = 0.75 and $\log(J(A\ cm^{-2}))$ = −4.68 (Fig. 2d). For all these SAMs, the supramolecular structure is essentially the same (Table 1) and therefore supramolecular effects can be ruled out. Across the dilution series, the currents at − 1.0 V are essentially constant (black dashed lines in Fig. 2), while the currents at + 1.0 V change by 2 orders of magnitude for X = -NH_2 and NO_2 (red dashed lines in Fig. 2) to give the measured rectification profiles (Fig. 3d). These observations imply that the van der Waals coupling between the Fc—X provides alternative intermolecular tunneling pathways.

Conclusions

In conclusion, our results show that large cooperative effects can result in alternative tunneling pathways in SAM-based junctions by adding small amounts (here 5–10%) of diluent to the SAM resulting in an increase of the off-resonant tunneling rate of two orders of magnitude. Here, we focused our efforts on a well-characterized tunneling junction based on $S(CH_2)_{11}Fc$ SAMs making it possible to ensure that the observed change in tunneling rates was not caused by structural disorder induced by the diluent. Besides tuning the electrical properties by varying the diluent concentration, we also demonstrated that the cooperative effect strongly depends on the strength of the van der Waals interaction between the diluent and the redox center of the SAM. Our experiments reveal that cooperative effects are important in the off-resonant tunneling regime, but are negligible in the incoherent tunneling regime, giving new insights into the experimental conditions under which cooperative effects can be expected. Our results indicate that cooperative effects can play a significant role in molecular junctions and could potentially provide an alternative way to design tunneling junctions and devices.

Funding

This work was supported by the Ministry of Education (MOE), Singapore, under award No. MOE2015-T2-1-050, the NUS core support grant no. C-380-003-003-001 and Science Foundation Ireland (SFI) under awards number 15/CDA/3491 and 12/RC/2275_P2.

CRediT authorship contribution statement

Yuan Li, Damien Thompson and Christian A. Nijhuis initiated the project and designed the experiments. Yuan Li and Dandan Wang prepared samples and conducted the electrical measurement. Dandan Wang, Li Jiang and Xiaojiang Yu performed surface characterization of samples. Dandan Wang and Wuxian Peng analyzed experimental data. Damien Thompson provided theory calculation. All authors contributed to the writing of the manuscript. All authors checked the manuscript and agreed to its submission. We confirm that this manuscript is the authors' original work. We confirm that this work has not been published nor is it being submitted simultaneously elsewhere.

Declaration of Competing Interest

The authors declare that they have no known competing financial interests or personal relationships that could have appeared to influence the work reported in this paper.

Acknowledgements

We acknowledge the Prime Minister's Office, Singapore under its Medium sized center program is also acknowledged for supporting this research. DT acknowledges support from Science Foundation Ireland (SFI) and supercomputing resources at the SFI/Higher Education Authority Irish Center for High-End Computing (ICHEC).

Appendix A. Supporting information

Supplementary data associated with this article can be found in the online version at doi:10.1016/j.nantod.2022.101497.

References

[1] A. Vilan, D. Aswal, D. Cahen, Large-area, ensemble molecular electronics: motivation and challenges, Chem. Rev. 117 (2017) 4248–4286.
[2] D. Xiang, X.L. Wang, C.C. Jia, T. Lee, X.F. Guo, Molecular-scale electronics: from concept to function, Chem. Rev. 116 (2016) 4318–4440.
[3] L. Sun, Y.A. Diaz-Fernandez, T.A. Gschneidtner, F. Westerlund, S. Lara-Avila, K. Moth-Poulsen, Single-molecule electronics: from chemical design to functional devices, Chem. Soc. Rev. 43 (2014) 7378–7411.
[4] S.V. Aradhya, L. Venkataraman, Single-molecule junctions beyond electronic transport, Nat. Nano 8 (2013) 399–410.
[5] D. Thompson, C.A. Nijhuis, Even the odd numbers help: failure modes of SAM-based tunnel junctions probed via odd-even effects revealed in synchrotrons and supercomputers, ACC Chem. Res. 49 (2016) 2061–2069.
[6] D. Thompson, Ed Barco, C.A. Nijhuis, Design principles of dual-functional molecular switches in solid-state tunnel junctions, Appl. Phys. Lett. 117 (2020) 030502.
[7] Y. Liu, X. Qiu, S. Soni, R.C. Chiechi, Charge transport through molecular ensembles: recent progress in molecular electronics, Chem. Phys. Rev. 2 (2021) 021303.
[8] R. Frisenda, D. Stefani, H.S.J. van der Zant, Quantum transport through a single conjugated rigid molecule, a mechanical break junction study, Accounts Chem, Res 51 (2018) 1359–1367.
[9] M.G. Reuter, M.C. Hersam, T. Seideman, M.A. Ratner, Signatures of cooperative effects and transport mechanisms in conductance histograms, Nano Lett. 12 (2012) 2243–2248.
[10] M.G. Reuter, T. Seideman, M.A. Ratner, Molecular conduction through adlayers: cooperative effects can help or hamper electron transport, Nano Lett. 11 (2011) 4693–4696.
[11] G.D. Kong, S.E. Byeon, S. Park, H. Song, S.-Y. Kim, H.J. Yoon, Mixed molecular electronics: tunneling behaviors and applications of mixed self-assembled monolayers, Adv. Elec. Mater. 6 (2020) 1901157.
[12] V. Obersteiner, G. Huhs, N. Papior, E. Zojer, Unconventional current scaling and edge effects for charge transport through molecular clusters, Nano Lett. 17 (2017) 7350–7357.
[13] Y. Selzer, L. Cai, M.A. Cabassi, Y. Yao, J.M. Tour, T.S. Mayer, D.L. Allara, Effect of local environment on molecular conduction: isolated molecule versus self-assembled monolayer, Nano Lett. 5 (2005) 61–65.
[14] M. Galperin, A. Nitzan, Cooperative effects in inelastic tunneling, J. Phys. Chem. B 117 (2013) 4449–4453.
[15] Z. Li, I. Franco, Molecular electronics: toward the atomistic modeling of conductance histograms, J. Phys. Chem. C. 123 (2019) 9693–9701.
[16] A. Kovalchuk, D.A. Egger, T. Abu-Husein, E. Zojer, A. Terfort, R.C. Chiechi, Dipole-induced asymmetric conduction in tunneling junctions comprising self-assembled monolayers, RSC Adv. 6 (2016) 69479–69483.
[17] X. Chen, B. Kretz, F. Adoah, C. Nickle, X. Chi, X. Yu, E. del Barco, D. Thompson, D.A. Egger, C.A. Nijhuis, A single atom change turns insulating saturated wires into molecular conductors, Nat. Commun. 12 (2021) 3432.
[18] M. Baghbanzadeh, L. Belding, L. Yuan, J. Park, M.H. Al-Sayah, C.M. Bowers, G.M. Whitesides, Dipole-induced rectification across Ag^{TS}/SAM//Ga_2O_3/EGaIn junctions, J. Am. Chem. Soc. 141 (2019) 8969–8980.
[19] J. Trasobares, J. Rech, T. Jonckheere, T. Martin, O. Aleveque, E. Levillain, V. Diez-Cabanes, Y. Olivier, J. Cornil, J.P. Nys, R. Sivakumarasamy, K. Smaali, P. Leclere, A. Fujiwara, D. Théron, D. Vuillaume, N. Clément, Estimation of π–π electronic couplings from current measurements, Nano Lett. 17 (2017) 3215–3224.
[20] Y. Dubi, Transport through self-assembled monolayer molecular junctions: role of in-plane dephasing, J. Phys. Chem. C. 118 (2014) 21119–21127.
[21] N. Nerngchamnong, L. Yuan, D.C. Qi, J. Li, D. Thompson, C.A. Nijhuis, The role of van der Waals forces in the performance of molecular diodes, Nat. Nanotechnol. 8 (2013) 113–118.
[22] A. Landau, A. Nitzan, L. Kronik, Cooperative effects in molecular conduction II: the semiconductor–metal molecular junction, J. Phys. Chem. A 113 (2009) 7451–7460.
[23] A. Landau, L. Kronik, A. Nitzan, Cooperative effects in molecular conduction, J. Comput. Theor. Nanos. 5 (2008) 535–544.
[24] C.E.D. Chidsey, C.R. Bertozzi, T.M. Putvinski, A.M. Mujsce, Coadsorption of ferrocene-terminated and unsubstituted alkanethiols on gold-electroactive self-assembled monolayers, J. Am. Chem. Soc. 112 (1990) 4301–4306.

[25] G.D. Kong, J. Jin, M. Thuo, H. Song, J.F. Joung, S. Park, H.J. Yoon, Elucidating the role of molecule–electrode interfacial defects in charge tunneling characteristics of large-area junctions, J. Am. Chem. Soc. 140 (2018) 12303–12307.
[26] G.D. Kong, M. Kim, S.J. Cho, H.J. Yoon, Gradients of rectification: tuning molecular electronic devices by the controlled use of different-sized diluents in heterogeneous self-assembled monolayers, Angew. Chem. Int. Ed. 55 (2016) 10307–10311.
[27] I. Katsouras, V. Geskin, A.J. Kronemeijer, P.W.M. Blom, D.M. de Leeuw, Binary self-assembled monolayers: apparent exponential dependence of resistance on average molecular length, Org. Electron. 12 (2011) 857–864.
[28] S. Kumar, J.T. van Herpt, R.Y.N. Gengler, B.L. Feringa, P. Rudolf, R.C. Chiechi, Mixed monolayers of spiropyrans maximize tunneling conductance switching by photoisomerization at the molecule–electrode interface in EGaIn junctions, J. Am. Chem. Soc. 138 (2016) 12519–12526.
[29] G.D. Kong, H. Song, S. Yoon, H. Kang, R. Chang, H.J. Yoon, Interstitially mixed self-assembled monolayers enhance electrical stability of molecular junctions, Nano Lett. 21 (2021) 3162–3169.
[30] H. Kang, G.D. Kong, H.J. Yoon, Solid state dilution controls marcus inverted transport in rectifying molecular junctions, J. Phys. Chem. Lett. 12 (2021) 982–988.
[31] R.C. Chiechi, E.A. Weiss, M.D. Dickey, G.M. Whitesides, Eutectic gallium–indium (EGaIn): a moldable liquid metal for electrical characterization of self-assembled monolayers, Angew. Chem. Int. Ed. 47 (2008) 142–144.
[32] L. Jiang, T. Wang, C.A. Nijhuis, Fabrication of ultra-flat silver surfaces with sub-micro-meter scale grains, Thin Solid Films 593 (2015) 26–39.
[33] N. Nerngchamnong, H. Wu, K. Sotthewes, L. Yuan, L. Cao, M. Roemer, J. Lu, K.P. Loh, C. Troadec, H.J.W. Zandvliet, C.A. Nijhuis, Supramolecular structure of self-assembled monolayers of ferrocenyl terminated n-alkanethiolates on gold surfaces, Langmuir 30 (2014) 13447–13455.
[34] T. Ikeda, K. Tahara, T. Kadoya, H. Tajima, N. Toyoda, S. Yasuno, Y. Ozawa, M. Abe, Ferrocene on insulator: silane coupling to a SiO_2 surface and influence on electrical transport at a buried interface with an organic semiconductor layer, Langmuir 36 (2020) 5809–5819.
[35] N. Nerngchamnong, D. Thompson, L. Cao, L. Yuan, L. Jiang, M. Roemer, C.A. Nijhuis, Nonideal electrochemical behavior of ferrocenyl–alkanethiolate SAMs maps the microenvironment of the redox unit, J. Phys. Chem. C. 119 (2015) 21978–21991.
[36] S. Lee, J. Park, R. Ragan, S. Kim, Z. Lee, D.K. Lim, D.A.A. Ohlberg, R.S. Williams, Self-assembled monolayers on Pt(111): molecular packing structure and strain effects observed by scanning tunneling microscopy, J. Am. Chem. Soc. 128 (17) (2006) 5745–5750.
[37] E. Laviron, Surface linear potential sweep voltammetry: equation of the peaks for a reversible reaction when interactions between the adsorbed molecules are taken into account, J. Electroanal. Chem. Interfacial Electrochem. 52 (1974) 395–402.
[38] H. Tian, Y. Dai, H. Shao, H.-Z. Yu, Modulated intermolecular interactions in ferrocenylalkanethiolate self-assembled monolayers on gold, J. Phys. Chem. C. 117 (2013) 1006–1012.
[39] A.V. Rudnev, K. Yoshida, T. Wandlowski, Electrochemical characterization of self-assembled ferrocene-terminated alkanethiol monolayers on low-index gold single crystal electrodes, Electrochim. Acta 87 (2013) 770–778.
[40] A.J.B. a L.R. Faulkner, Electrochemical Methods - Fundamentals and Applns, second ed., Wiley,, New York, 2001.
[41] W.F. Reus, C.A. Nijhuis, J.R. Barber, M.M. Thuo, S. Tricard, G.M. Whitesides, Statistical tools for analyzing measurements of charge transport, J. Phys. Chem. C. 116 (2012) 6714–6733.
[42] C.A. Nijhuis, W.F. Reus, J.R. Barber, M.D. Dickey, G.M. Whitesides, Charge transport and rectification in arrays of SAM-based tunneling junctions, Nano Lett. 10 (2010) 3611–3619.
[43] S. Grimme, Density functional theory with London dispersion corrections, WIREs Comput. Mol. Sci. 1 (2011) 211–228.